Available online at www.sciencedirect.com
SCIENCE DIRECT®
Journal of Chromatography A, 1049 (2004) 115–125
JOURNAL OF CHROMATOGRAPHY A
www.elsevier.com/locate/chroma

Characterisation by high-performance liquid chromatography–multiple mass spectrometry of intermediate compounds formed from mepanipyrim photoinduced degradation

Paola Calza[a,*], Claudio Medana[a], Claudio Baiocchi[a], Paolo Branca[b], Ezio Pelizzetti[a]

[a] *Department of Analytical Chemistry, University of Torino, Via P. Giuria 5, 10125 Torino, Italy*
[b] *Agenzia Regionale Protezione Ambientale, Polo Regionale Alimenti, Via Nizza 24, La Loggia (TO), Italy*

Received 29 March 2004; received in revised form 23 July 2004; accepted 26 July 2004
Available online 28 August 2004

Abstract

Mepanipyrim, a widely used pyrimidinic fungicide, has been photocatalytically degraded in aqueous solution on TiO_2. The purpose of this study is to artificially produce degradation compounds similar to those formed in the environment. Numerous intermediates have been identified and characterised through a MS^n spectra analysis, allowing us to give insight into the early steps of the degradation process. Several concomitant pathways occur concerning both reductive and/or oxidative attacks; the main steps involve the cleavage of triple bond, mono and bihydroxylation of the parent molecule, loss of benzene moiety and/or propynylic chain. All these structures are easily degraded themselves, so that the only species recognised to endure in the investigated times is guanidine. A mechanism of transformation accounting for the identified intermediates is proposed.

Keywords: Mepanipyrim; Titanium dioxide; Guanidine

1. Introduction

Mepanipyrim (*N*-(4-methyl-6-prop-1-ynilpyrimidin-2-yl) aniline) is a fungicide widely adopted in agriculture [1–3] and that has recently shown interesting application in pharmacology [4]. It may be of concern the identification of possible degradation products, coming from mepanipyrim transformation, so long to research them along with the parent molecule in real samples. At present, only few metabolic studies are available about its transformation; metabolic studies carried out in soil and tomato seedlings show 2-(4-methyl- 6- (1- propynyl) pyrimidin- 2- ylamino)phenol, 4-(4-methyl- 6-(1- propynyl)pyrimidin- 2-ylamino) phenol, 1-(2-anilino-6-methyl pyrimidin-4-yl)-2-propanol, 1-(2-anilino-6-methyl pyrimidin-4-yl)-2-propan-one and 4-methyl-6-(1-propynyl) pyrimidin-2-ylamine as products [1,2].

However, some more information about its transformations may be obtained adopting a photocatalytic degradation. The feasibility of this laboratory simulation has been successfully applied in previous studies [5,6] and could be similarly utilised in the present conditions, such enlighting the photoinduced mechanism involving mepanipyrim degradation.

Photocatalytic degradation with irradiated semiconductors [7–12] has been established to be effective for degradation and final mineralisation of several organic compounds and in gaining information on naturally occurring transformations. The basic principles of heterogeneous photocatalysis processes have been extensively discussed elsewhere [13–15] and are here only briefly presented. The primary photochemical event, following the near-UV light adsorption by TiO_2 ($\lambda < 380$ nm), is the generation of electron/hole pairs in the bulk of the semiconductor. The charge carriers can either recombine or migrate to the surface where they are ultimately

* Corresponding author. Tel.: +39 011 6707626; fax: +39 011 6707615.
E-mail address: paola.calza@unito.it (P. Calza).

0021-9673/$ – see front matter © 2004 Elsevier B.V. All rights reserved.
doi:10.1016/j.chroma.2004.07.055

trapped, the electrons as Ti(III) and the holes as surface radical hydroxyl group. If electrons acceptor or electron donors are present at the surface, interfacial electron transfer may occur.

The oxidising species may be holes (h^+_{VB}, more oxidising than aqueous hydroxy radical), trapped holes (less oxidising than aqueous hydroxy radical) or hydroxy radicals [15,16]; the reducing species may be conduction band electrons (e^-_{CB}) or trapped electrons, both less reducing than aquated electrons [13,17,18]. Whether a process takes place under photocatalytic conditions is related to the redox property of e^-_{CB} and h^+_{VB} on the one part and organic compounds on the other. Considering that oxidative and reductive photocatalytic processes are operating and that the presence of oxygen adds further and alternative degradation pathways, we have characterised the photocatalysed transformation products through an accurate analysis of the MS/MS spectra.

2. Experimental section

2.1. Material and reagents

Mepanipyrim (Aldrich) and guanidine (Aldrich) were used as received. Sodium sulphate (Aldrich), ammonium chloride (Carlo Erba), potassium nitrate (Merck) and sodium nitrite (Carlo Erba) were used after drying. HPLC grade water was obtained from MilliQ System Academic (Waters, Millipore). Methanol HPLC grade (BDH) was filtered through a 0.45 μm filter before use. Ammonium acetate reagent grade was purchased from Fluka.

All experiments were carried out using TiO_2 Degussa P25 as the photocatalyst. In order to avoid possible interference from ions adsorbed on the photocatalyst, the TiO_2 powder was irradiated and washed with distilled water until no signal due to chloride, sulphate or sodium ions could be detected by ion chromatography.

2.2. Irradiation procedures

The irradiations have been performed using a 1500 W xenon lamp (Solarbox, CO.FO.MEGRA, Milan, Italy) simulating AM1 solar light and equipped with a 340-nm cut-off filter. The total photons flux (340–400 nm) in the cell and the temperature during irradiation has been kept constant for all experiments. Those were 1.35×10^{-5} Einstein min^{-1} and 50 °C, respectively. The irradiation was carried out on 5 ml of suspension containing 15 mg L^{-1} mepanipyrim and 200 mg L^{-1} TiO_2. The entire content of the cell was filtered through a 0.45 μm filter and then analysed by an HPLC–MS instrument and a ionic chromatographer.

2.3. Analytical procedures

2.3.1. Liquid chromatography

The chromatographic separations were run on a C18 column Varian Polaris, 150 mm × 2.0 mm (Chrompack, The Netherlands). Injection volume was 10 μL and flow rate was 200 μL min^{-1}. Gradient mobile phase composition was adopted: 0/100 to 30/70 in 25 min methanol/aqueous ammonium acetate 15 mM pH 6.8.

2.3.2. Mass spectrometry

A LCQ DECA XP Plus ion trap mass spectrometer (ThermoFinnigan) equipped with an atmospheric pressure interface and an ESI ion source was used. The LC column effluent was delivered into the ion source using nitrogen as sheath and auxiliary gas (Claind Nitrogen Generator apparatus). The source voltage was set at the 4.5 kV value. The heated capillary value was maintained at 300 °C. The acquisition method used was previously optimised in the tuning sections for the parent compound (capillary, magnetic lenses and collimating octapoles voltages) in order to achieve the maximum of sensitivity. The tuning parameters adopted for ESI source have been the following: source current 5.00 μA, capillary voltage 11.00 V, capillary temperature 300 °C, tube lens −20 V; for ions optics, multipole 1 offset −6.75 V, inter multipole lens voltage −16.00 V, multipole 2 offset −10.50 V.

2.3.3. Ion chromatography

A Dionex instrument has been employed equipped with a conductimeter detector. The determination of ammonium ions has been performed by adopting a column CS12A and 25 mM metansulphonic acid as eluant, flow rate of 1 ml min^{-1}. In such conditions, the retention time is 4.7 min. The anions have been analysed by using a AS9HC anionic column and a mixture of $NaHCO_3$ 12 mM and K_2CO_3 5 mM at a flow rate of 1 ml min^{-1}. In such experimental conditions the retention times are 6.63 min, 9.58 min for nitrite and nitrate, respectively.

2.3.4. Total carbon analyser

Total organic carbon (TOC) was measured on filtered suspensions using a Shimadzu TOC-5000 analyser (catalytic oxidation on Pt at 680 °C). Calibration was achieved by injecting standards of potassium phthalate.

3. Results and discussion

3.1. Mepanipyrim

The disappearance of mepanipyrim and the intermediates evolution have been accurately monitored by HPLC–MS^n analysis of solutions after various irradiation times. The primary compound is rapidly degraded through a pseudo-first order decay and it is completely disappeared until 15 min of irradiation, as assessed in Fig. 1.

The parent molecule of mepanipyrim elutes at 18.12 min and exhibits a quasi-molecular ion at *m*/*z* 224 as base peak. Several peculiar fragments have been extracted from the MS^2 spectrum (see Table 1 and Fig. 2) and are linked together through the fragmentation pathway proposed in the inset in Fig. 2.

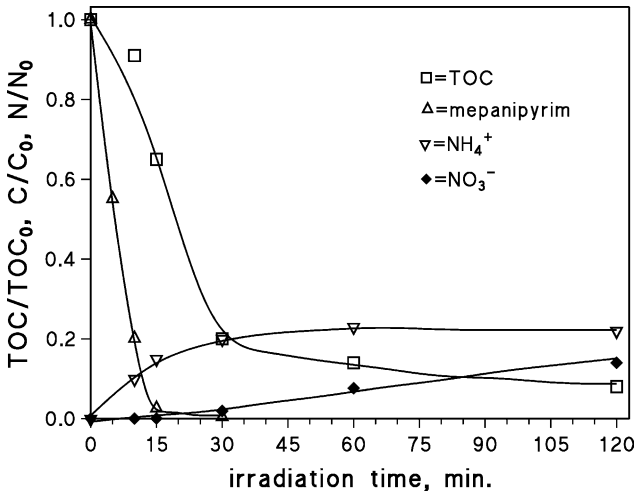

Fig. 1. Degradation of mepanipyrim 15 mg L^{-1} on TiO_2 200 mg L^{-1}; disappearance of initial compound, TOC profile and evolution of ammonium and nitrate ions.

It is worth noting that mepanipyrim is a particularly stable molecule difficult to fragment, so that high collision energy have been required. Such elevated stability is certainly due to the extended conjugated system that exhibits usually deactivated fragmentation pathways, such as the loss of a methyl radical from the parent molecule with the formation of radical ion at *m/z* 209, prevailing over neutral molecules losses, such as aniline (*m/z* 131). In addition, the cleavage of C–N and C–C bonds occurs with release of a MeCN molecule (fragment *m/z* 183) and the loss of ammonia, involving heavy rearrangement of the rest of the structure with the formation of *m/z* 207. This fragmentation pathway will be carefully considered in identifying the unknown intermediates.

Table 1
Main fragments coming from MS and MS^n spectra of the species represented in Scheme 4

		MS^2 fragments	MS^3 fragments
m/z 224	t_R = 18.12 min	209	194, 182
		207	192
		183	157
		160	–
		131	104
m/z 240	(1) t_R = 13.29 min	212	–
		223	197
		225	198, 197, 145
	(2) t_R = 14.70 min	223	195
		225	208
		199	–
	(3) t_R = 15.86 min	223	196, 143
m/z 256	(4) t_R = 10.31 min	228	–
		239	211
	(5) t_R = 12.36 min	228	–
		239	221
	(6) t_R = 13.00 min	239	211, 221
		215, 228	–
m/z 238	(7) t_R = 9.86 min	221	162, 192, 203
m/z 254	(8) t_R = 9.67 min	–	–
m/z 186	(9) t_R = 2.69 min	169, 130	–
m/z 202	(10 and 11) t_R = 6.04 min	185	167
		160	–
m/z 218	(12) t_R = 4.06 min	201	–
	(13) t_R = 5.42 min	201	–
m/z 164	(14) t_R = 4.16 min	107	–
m/z 148	(15) t_R = 8.59 min	131	104
		91	–
m/z 126	(16) t_R = 2.69 min	108, 109	–

3.2. Intermediates characterisation

As well as the mepanipyrim photocatalysed degradation is achieved, numerous intermediates have been identified (Fig. 3). As arises from Figs. 4–6, various species have been recognised, characterised by different *m/z* ratios along with several peaks corresponding to an equal *m/z* value. The compounds holding *m/z* 240, 242 and 244 are initially formed in a relevant yield, so pointing out they represent the key products in the early mepanipyrim transformation steps. Besides, their simultaneous formation can be considered as a proof of their production through different initial mechanisms.

A closer inspection reveals three peaks at *m/z* 240, whose formation and disappearance kinetics are shown in Fig. 4. All of them present retention times shorter than mepanipyrim; it would seem reasonable to assign them the structure of the hydroxylated mepanipyrim. More than one derivative is simply the consequence of the non-selectivity of the $^{\bullet}OH$ radical attack. Carbon-centred radicals generated by hydroxyl radical attacks may react with O_2 to give organoperoxy radicals ($ROO^{\bullet}$) which can decompose to form $^{\bullet}HO_2$ or, ultimately, non-radical oxygenated products [19,20].

Their MS^2 and MS^3 peculiar fragments are presented in Table 1 (structure labelled 1–3). By comparing them with those coming from mepanipyrim, several analogies/differences come up and they are useful in attributing the position for $^{\bullet}OH$ radical attack. From the MS^n evidences, structure 1 presents a CH_3 radical loss (*m/z* 225), so excluding the hydroxylation on the propynylic chain. In addition, the concomitant absence of MeCN loss (*m/z* 199) implies that the OH attack probably occurs in the pyrimidinic moiety.

Specularly, structure 2 presents both methyl radical and MeCN losses, so excluding either the attack on lateral chain or on the pyrimidinic ring. We are moved to conclude that the hydroxylation occurs on the benzenic ring, probably in ortho or para position, so giving the formation of 2-(4-methyl-6-(1-propynyl)pyrimidin-2-ylamino)phenol and/or 4-(4-methyl-6-(1-propynyl)pyrimidin-2-ylamino)phenol, similarly to what was already been found in metabolic studies [1–3]. In structure 3, the absence of the methyl radical loss suggests that the hydroxylation occurs on the propynylic chain.

Even if the available information is not enough to unequivocally attribute the points of attack, a confirmation of the assumed structures comes from the intermediates formed during the successive degradation pathways, as clarified below.

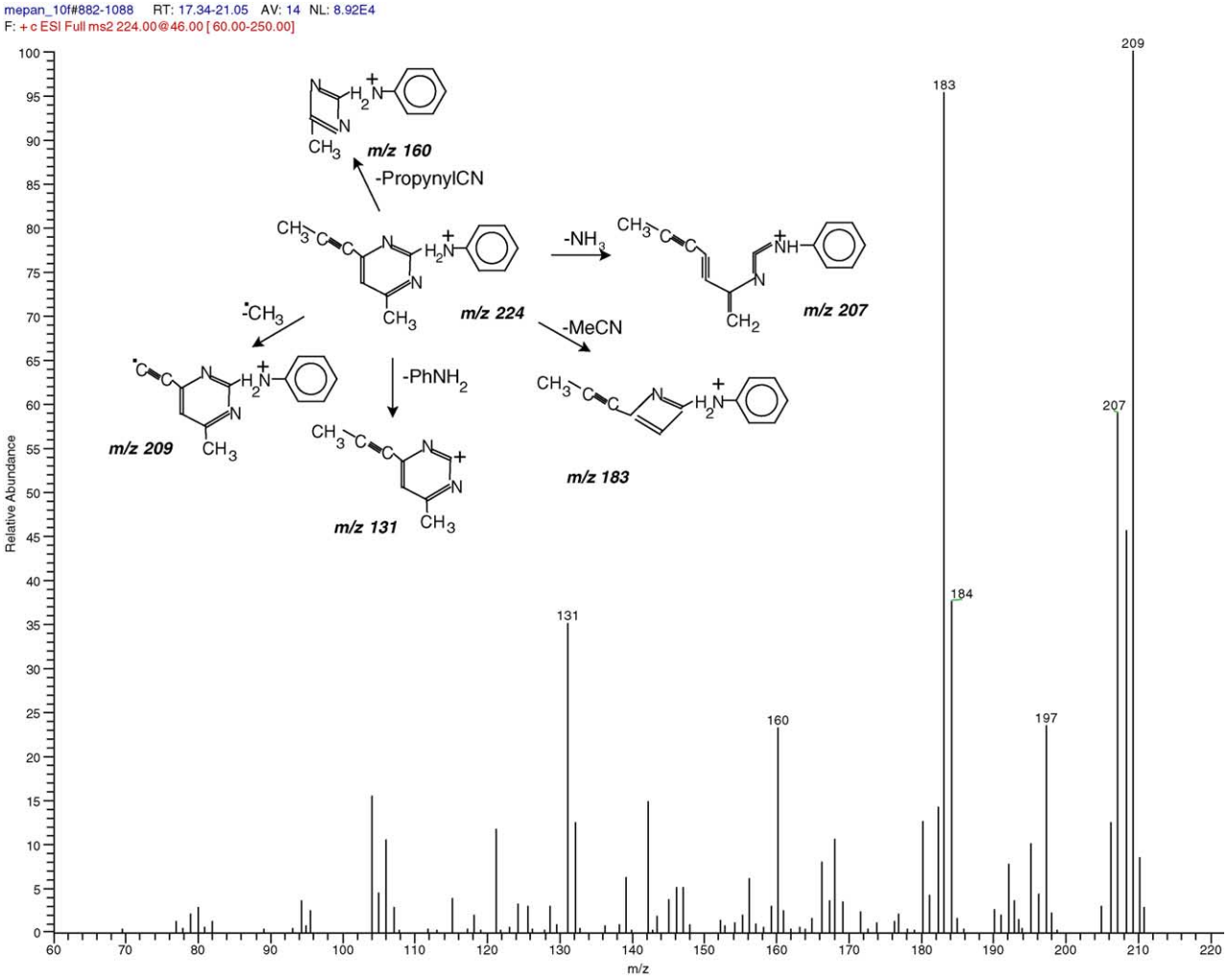

Fig. 2. MS^2 spectrum and, in inset, main fragmentation pathway followed by mepanipyrim (*m*/*z* 224).

Concurrently to structures 1–3 formation, three peaks having a *m*/*z* ratio of 256 and retention times slightly decreased in respect to species at *m*/*z* 240 (Fig. 4) have been detected and can be attributed to bihydroxylated derivatives. This type of oxidation rapidly occurs, as results by comparing their evolution kinetics with those only slightly delayed for the *m*/*z* 240 species. The fragmentation pattern observed from MS^n analysis (Table 1, structures 4–6) completely supports the supposed structures. The absence of methyl radical loss in species 5 and 6 is an indication about the hydroxylation of the methyl group on the propynylic chain; while the absence of MeCN loss evidenced in the structures 4 and 5 suggests hydroxylation on the heteroaromatic ring, the second OH group in 4 and 6 is probably located in the benzenic moiety.

At comparable times, the formation of molecules holding *m*/*z* 238 and 254 can be seen (Fig. 4 and Table 1, structures 7 and 8). It is in agreement with the alcoholic group oxidation into an aldehydic one. The loss of 29 amu endorses the presence of an aldehydic group, formable only from the oxidation of the alcoholic group of the lateral chain (see structure 7), so arising a further confirmation about the involvement of the lateral chain. Similarly, it could be formed the structure at *m*/*z* 254.

All these molecules seem to be degraded through several transformation pathways involving (1) the cleavage of C–C bond with the release of the propynylic chain and/or (2) cleavage of C–N bond with the detachment of benzenic moiety as phenol, hydroquinone or cathecol. These molecules are summarised in Fig. 6. Looking closely at the first pathway, the formation of different species, holding *m*/*z* 186 (structure 9), *m*/*z* 202 (structure 10 and 11) and *m*/*z* 218 (structure 12 and 13) is achieved. For the species 10–13, it is observed as main fragment the one showing a difference of 42 amu, with associated loss of ketene. It implies that, as discussed above, an OH group is located in the pyrimidinic moiety; they can be attributed to structures coming from the transformation of monohydroxylated (10 and 11) and bihydroxylated (12 and 13) derivatives. Similarly, through the cleavage of propynylic chain, the structure 7 is transformed into structure 9.

In parallel to the described pathways, the degradative process of the structures with *m*/*z* 256 yields, through the loss of the benzenic ring, to *m*/*z* 164 (structure 14 coming from

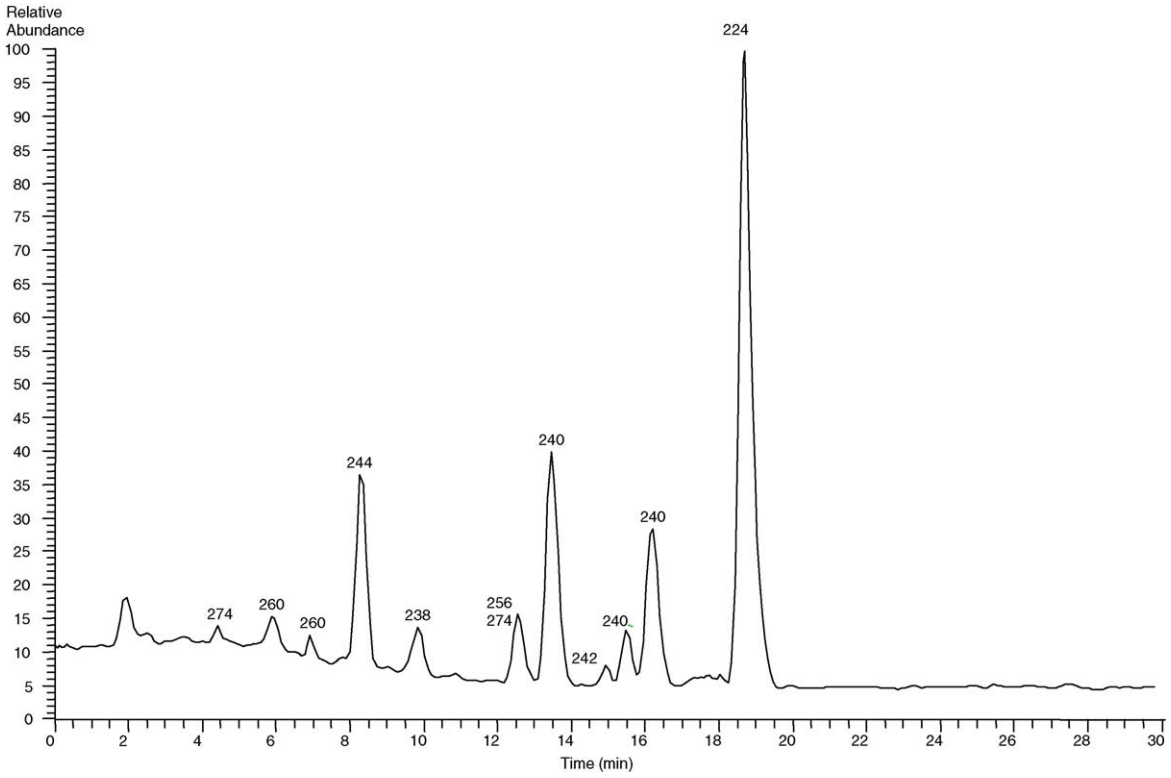

Fig. 3. Chromatographic profile of the solution at 10 min of irradiation showing the *m/z* of the main intermediates generated from mepanipyrim degradation.

structure 4) and *m/z* 148 (structure labelled 15 and coming from structure 2). A difference of 16 amu is imputable to the loss of a phenol group instead of benzene moiety, so endorsing the presence of an OH group in the benzenic ring in structure 2. By an accurate MS analysis emerges that all these species present the loss of ammonia (17 amu) and of guanidinic moiety (difference of 57 amu), in agreement with the detachment of the benzenic ring; no other significant fragments have been observed.

Structure at *m/z* 126 (see Table 1, labelled 16) could be formed through the concomitant occurrence of both pathways or from the loss of the benzenic moiety from the species 10 and 12. The MS spectrum indicates the loss of 18 (a molecule of water), as a signal about the persistence of an OH group on the heteroring.

Anyway, the degradation products described above represent only one of the possible transformation routes. An alternative pathway arise from the concerted oxidative and

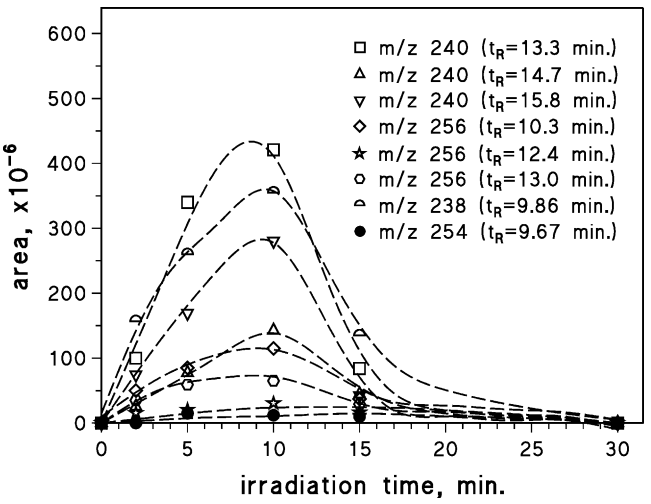

Fig. 4. Main intermediates generated from mepanipyrim degradation through an initial oxidative step.

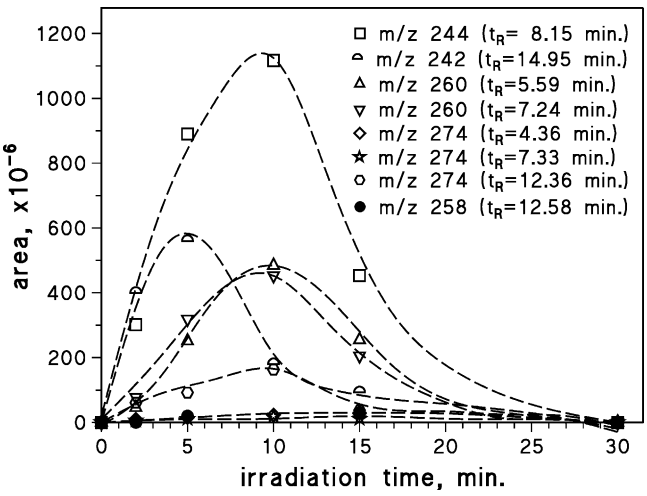

Fig. 5. Main intermediates generated from mepanipyrim degradation through an initial oxido/reductive sequence.

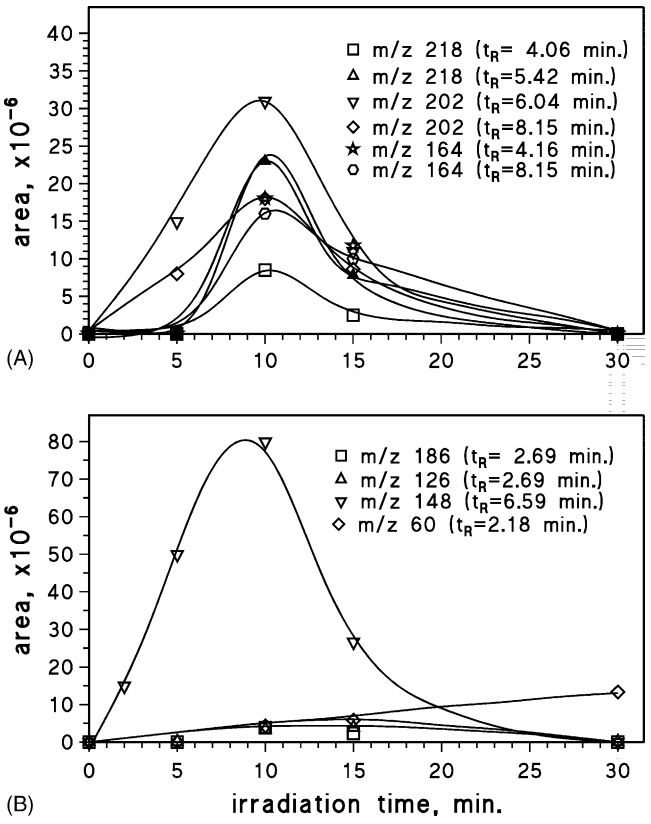

Fig. 6. Intermediates formed from mepanipyrim through successive degradation steps.

reductive attacks and leads to the formation of a peak holding *m/z* 244 (see Table 2 and Fig. 5). Its kinetic evolution is ever quicker than that of the species at *m/z* 240, as can be seen by comparing Figs. 4 and 5, so underlining their simultaneousness. The difference in amu in respect to the parent molecule is in favour to the concomitant attack of radical

Table 2
Main fragments coming from MS and MS^n spectra of the species represented in Scheme 5

		MS^2 fragments	MS^3 fragments
m/z 244	(18) t_R = 8.15 min	202	185, 160, 118, 84
m/z 242	(19) t_R = 14.48 min	224	–
		200	–
		186	–
		214	–
m/z 260	(20) t_R = 5.59 min	242	198
		218	176, 201, 84
		202	160, 185
	(21) t_R = 7.24 min	218	190, 148
		202	135, 184
		225	–
m/z 258	(22) t_R = 13.01 min	241	–
		242	–
		216	–
m/z 274	(23) t_R = 12.36 min	230	213, 187, 171
		256	228
	(24) t_R = 18.42 min	256	228
		202	185, 119, 84

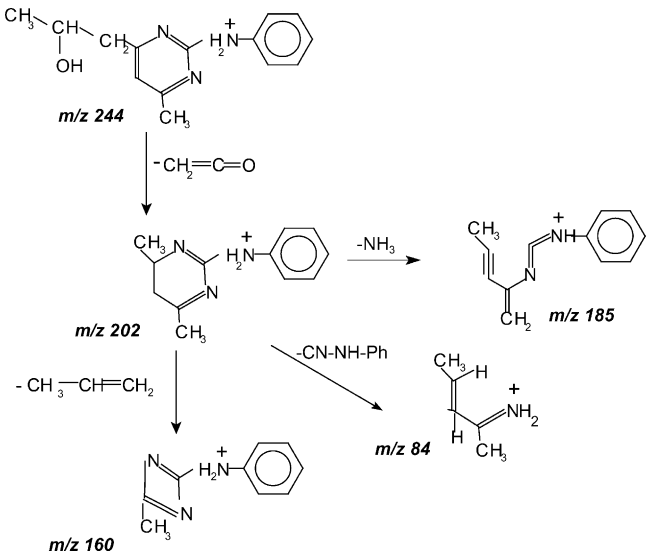

Scheme 1. Fragmentation pathway followed by the molecule at *m/z* 244.

•OH and electrons on the triple bond. The MS^2 and MS^3 formed ions (Table 2, structure labelled 18) may implicate a fragmentation pathway as indicate in Scheme 1.

Owing to the described pathway, we are then moved to conclude that OH radical attacks on C^2 on the propynylic chain, so assuming the formation of the species at *m/z* 244 (labelled 18). The same structure, 1-(2-anilino-6-methylpyrimidin-4-yl)-2-propanol, has been observed from mepanipyrim transformation in soil and tomato seedlings [1–3].

A species at *m/z* 242 has been initially seen in great amount (structure 19 in Table 2 and Fig. 4); it could be formed through the oxidation of the alcoholic group into an aldehydic one, as well as evidences in metabolic studies [1–3]. Nevertheless, this structure is in equilibrium with its tautomeric form, holding the double bond formalised between C^1 and C^2. A confirmation about the supposed structure comes from the MS^2 spectrum; it presents a loss of 42 (same pathway as *m/z* 244), loss of 28 (associated to CO) and 18 (loose of a water molecule from the enolic form). With this assumption, this structure could be formed directly from mepanipyrim (enolic form) or, otherwise, from the oxidation of structure *m/z* 244 (keto form). Its kinetic of formation is in favour to the first supposed attack.

The concomitance of two •OH radical and electrons attack leads to the formation of two molecules at *m/z* 260. By considering structures 20 and 21 from their MS^2 spectra, a loss of ketene and hydroxy-acetaldehyde leading to *m/z* 202 and 218 have been observed in both cases. In an effort to clarify the possible points of radical attack on the molecule, we have careful examined the MS^3 fragments. Instead the formation of the same fragments from the parent molecule, interesting differences come up from their peculiar daughter ions (see Scheme 2). By considering structure 20, the fragmentation pathway in Scheme 2A seems to be followed, so

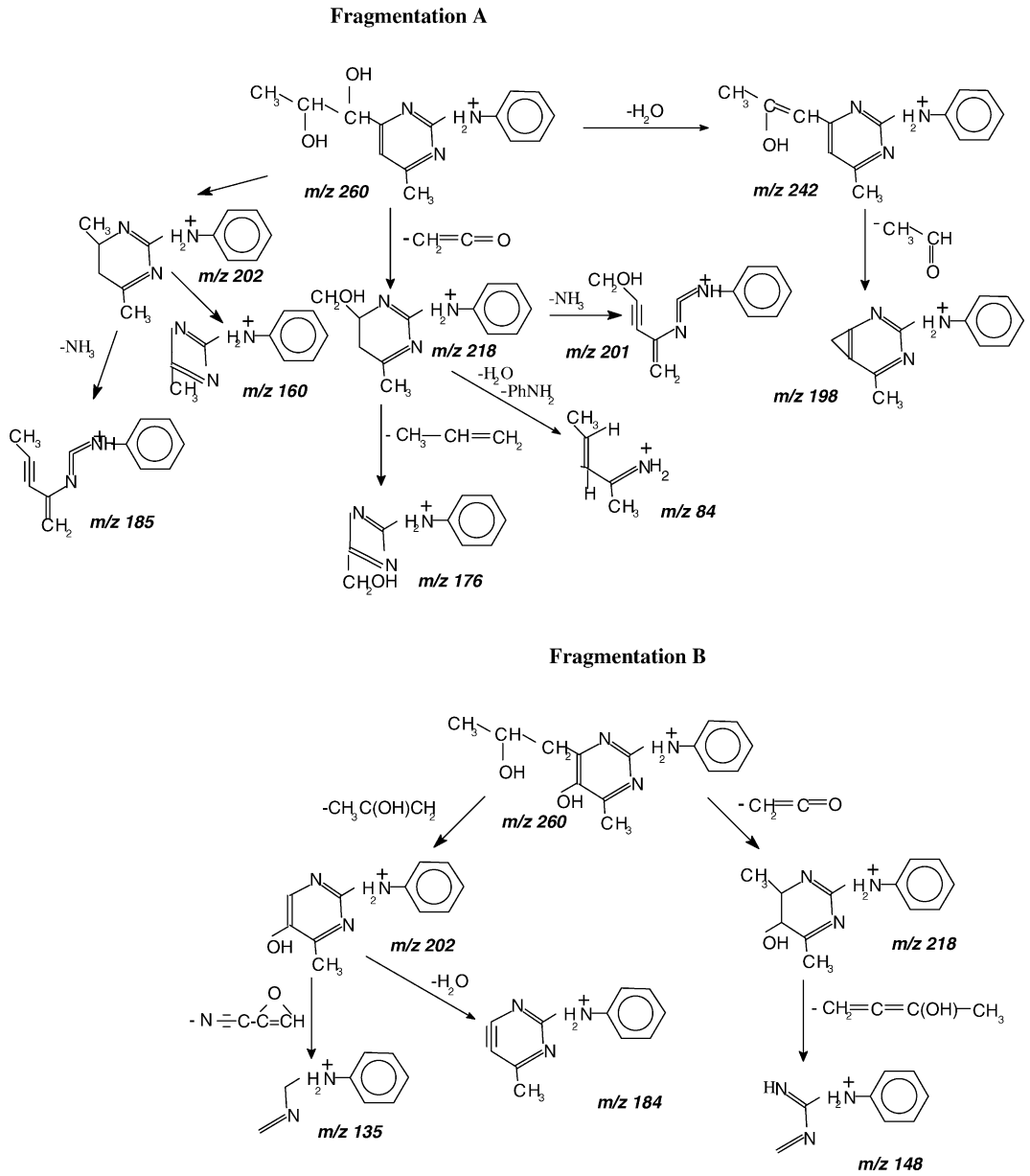

Scheme 2. Fragmentation pathways followed by the molecules holding *m*/*z* 260.

implicating the location of both OH groups in the propynylic chain. It can be rationalised through the formation, from *m*/*z* 202, to the identical fragments evidenced from *m*/*z* 244, and from *m*/*z* 218 to the same fragments as above plus an oxygen atom. Moreover, the fragmentation of *m*/*z* 242 leads to *m*/*z* 198 through the loss of acetaldehyde.

In a different way, the daughter ions formed from *m*/*z* 202 for structure 21 presents *m*/*z* 184 (loss of a water molecule) and *m*/*z* 135, so indicating an OH group is still present. The occurrence of a fragmentation pathways depicted in Scheme 2B lets us conclude that the additional OH radical attack occurs on the pyrimidinic ring.

A peak at *m*/*z* 258, correspondent to the keto-derivative, is also observed (see molecule 22 in Table 2). The presence of the same losses observed for structure 20 implies that the oxidation occurs on the propanolic chain.

A competitive pathway leads to the formation of two structure at *m*/*z* 274, labelled 23 and 24, through the oxidation of the alcoholic group and a further OH radical attack. The structure 23 probably follows a fragmentation pathway like the one proposed in Scheme 3A. The location of the three OH groups in the propynylic chain is supported by the MS^n evidences; in MS^2 spectrum a water molecule (*m*/*z* 256) and hydroxymethylketene (*m*/*z* 202) have been observed as peculiar losses. The MS^3 fragmentation has been performed on both ions; their daughter ions, formed through the Scheme 3A, assess the location of all the OH attacks on the lateral chain.

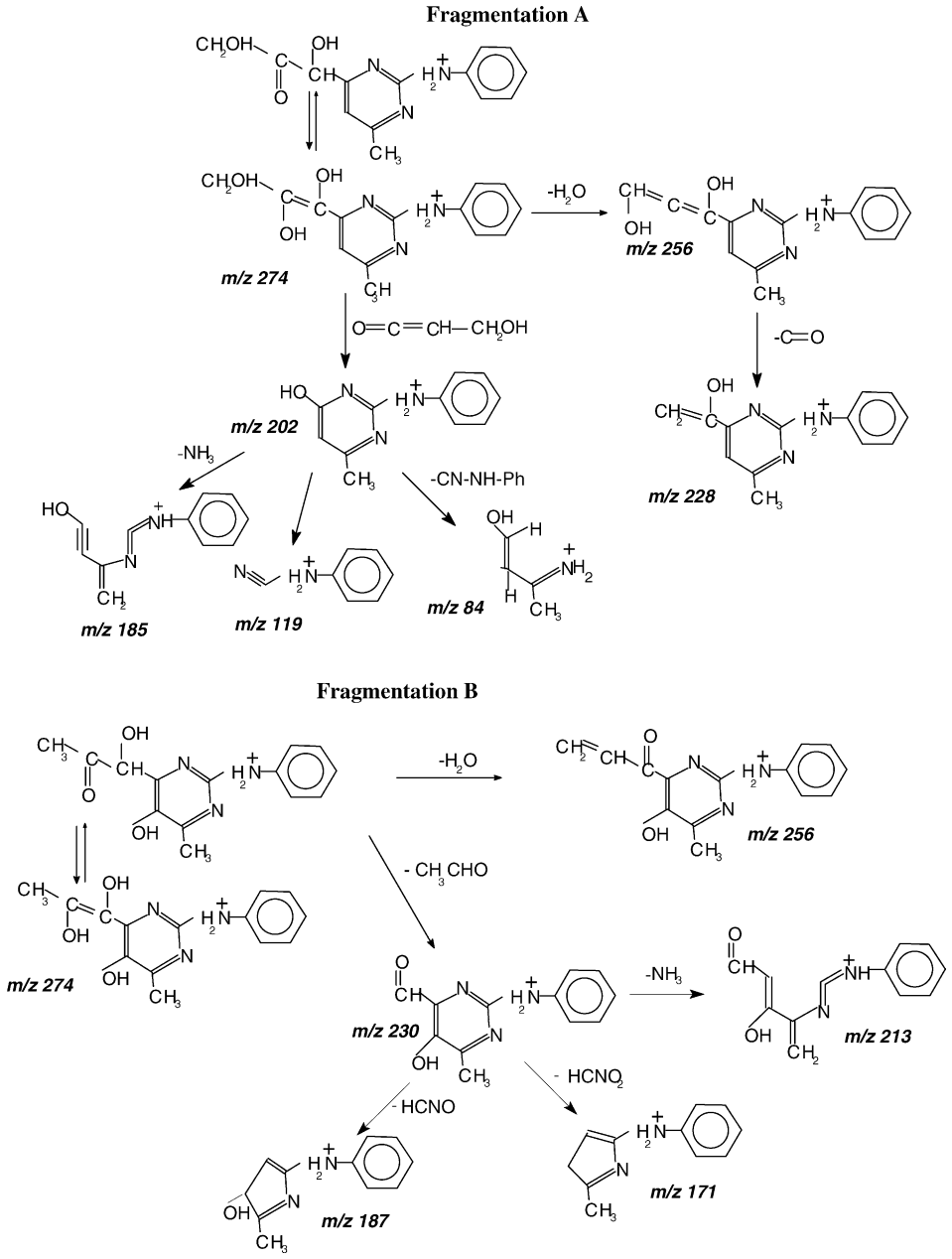

Scheme 3. Fragmentation pathways followed by the molecules holding *m*/*z* 274.

Structure 24, as assessable through Scheme 3B, hold the additional OH group on the pyrimidinic ring and a keto-group formation on C^2.

3.3. Mechanism of mepanipyrim photodegradation

Taking into account the identified intermediates described above, their kinetic evolution and their distribution, they can be linked together through the pathways described in Schemes 4 and 5. The transformation can initially proceed through an oxidative process, with the formation of the hydroxylated intermediates described in Scheme 4, whose active species is assumed to be the surface bound (or homogeneous) ·OH radical, or through an oxido/reductive sequence on the triple bond, catalysed by the e^-_{CB} and/or surface electrons on one side and OH addition on the other side, so forming the species illustrated in Scheme 5.

Looking closely at the Scheme 4 and owing to the precedent discussion, the first degradation step involves the formation of several hydroxy- and bihydroxy-mepanipyrim. Afterwards, various competitive pathways could occur so leading to a wide range of intermediates.

By considering hydroxymepanipyrim (1), in competition to the bihydroxy-derivatives formation (4 and 5), it can underwent the cleavage of lateral chain, so leading to the formation of a structure with MW 201 (10) or, through benzenic loss,

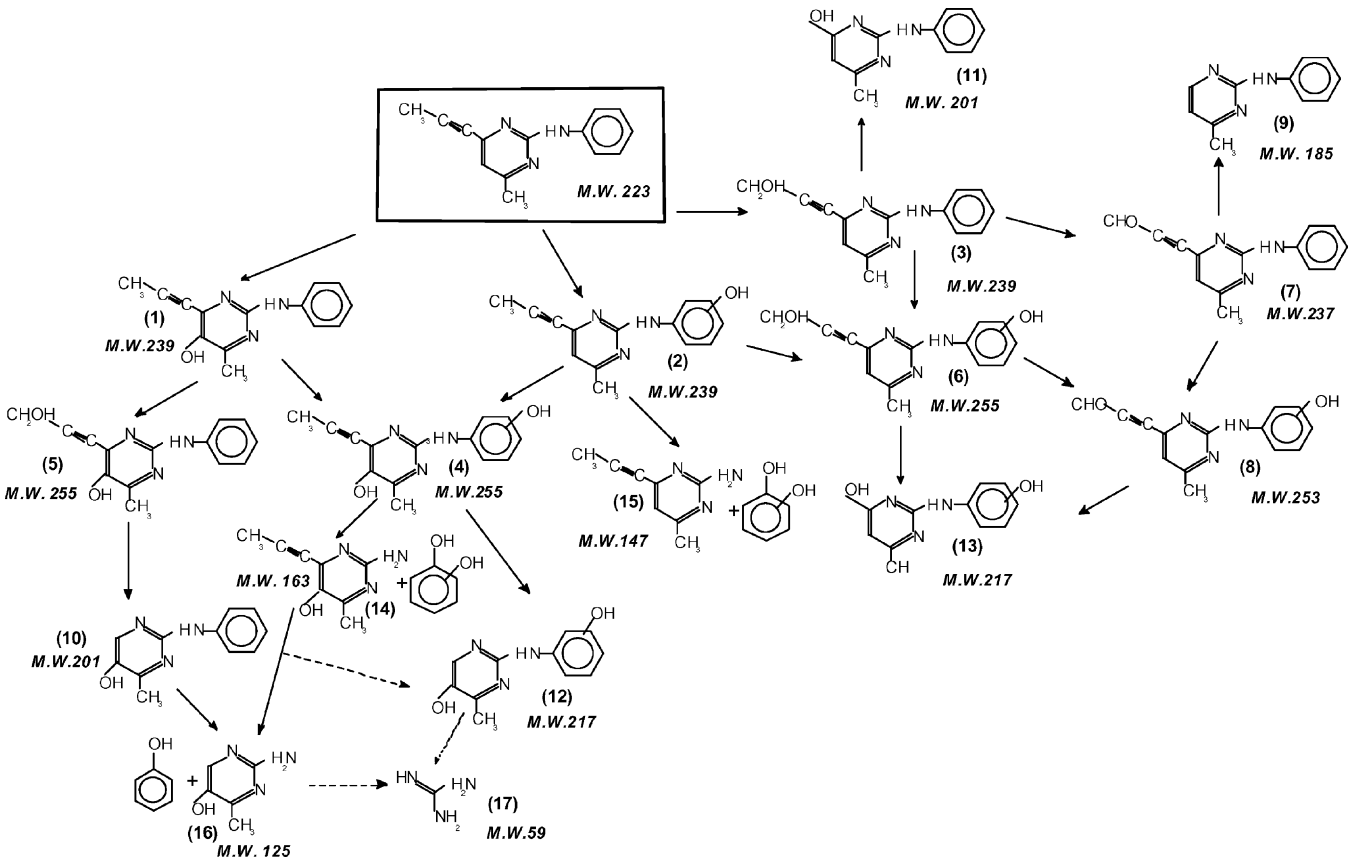

Scheme 4. Mepanipyrim degradation pathways initiated by oxidative attacks.

to the molecule with MW 163 (14); by the contemporaneous occurrence of both attacks can be formed the structure at MW 125 (16); all these compounds could be similarly produced from the degradation of bihydroxy-mepanipyrim (4 and 5). It is also worth noting that phenol, catechol and hydroquinone have been identified, so remarking the release of the aromatic ring occurs.

The transformation pathways occurring on hydroxymepanipyrim (2) could lead on one side to the bydroxylated derivative labelled 4 or 6 and, on the other side, to the structure at MW 147 (15), through the cleavage of C–N bond with the detachment of the phenolic moiety.

Likewise, the bihydrolylated derivative formation (5 and 6), could be formed from hydroxymepanipyrim (3). The alcoholic group can be easily oxidised into aldehydic group, so forming structures (7) and (8). Otherwise, through the detachment of propynylic chain from both hydroxy- and keto-mepanipyrim, the structures at MW 201 (11) and 185 (9) can be formed or, from the bihydroxyderivate (6) to the structure with MW 201 (labelled 13).

For all the illustrated species, the successive degradation steps lead to the formation of guanidine. Kinetically, it is the last species formed as noticeable in Fig. 6 and it is persistently observed in the considered time, in agreement with the high photocatalytic stability evidenced in previous studies [21].

By analysing the species enclosed in Scheme 5, a closer inspection of Fig. 5 reveals that the formation of species at MW 243 (18) and 241 (19) occurs at comparable rate. Their simultaneousness is in favour to the occurrence of two initial pathways leading, through the cleavage of the triple bond, to the formation of a double bond (holding an OH group) on one side and single bond in the other side.

Instead the formation of these species, the bihydroxylation process with the formation of two species at MW 259 (20 and 21) is realised, similarly to what observed above. In addition, a further OH attack can lead to the structure at MW 273 (23 and 24). By considering the fate of structure (21), it could yield to the formation of the molecule at MW 273 (23) passing through the formation of structure at MW 257, holding the keto-group instead the alcoholic one, or directly, through a further OH radical attack on the propanolic chain followed by the oxidation of an alcoholic group into a keto-group.

Nevertheless, being the reductive steps confined to the propynylic chain, further processes could occur in agreement to the pathways proposed in Scheme 4 with the formation of other aromatic structures, through the release of lateral chain and/or the benzenic ring.

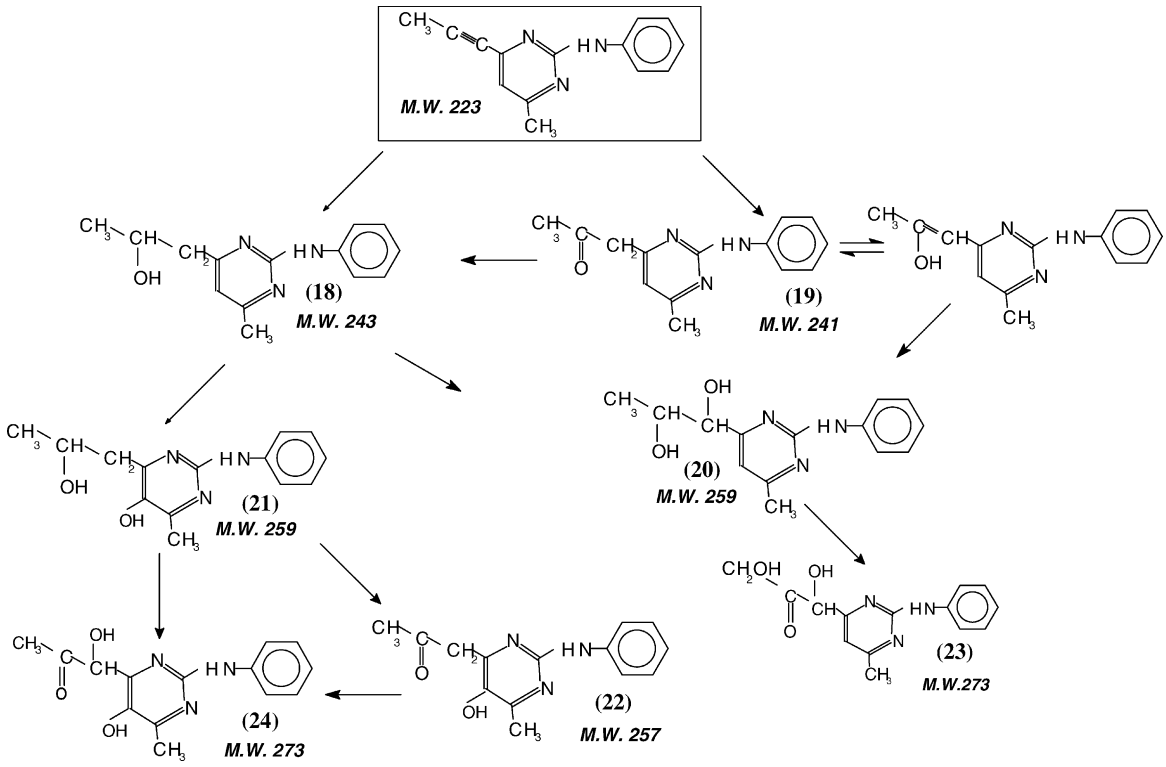

Scheme 5. Mepanipyrim degradation pathways initiated by oxido/reductive attacks.

3.4. Final products

All the identified structures are completely degraded until 30 min of irradiation. As far as aromatic intermediates degradation is concerned, TOC profile shows a remarkable decrease until 30 min (Fig. 1), while a small yield of organic carbon is persistently observed also after 120 min of irradiation, predominantly attributable to the guanidine formation. In the investigated time, as well as the organic carbon is mostly transformed into CO_2, a large amount of the organic nitrogen results still bound. Only a small yield has been released, mainly as ammonium ions, through a widely studied mechanism [21–28], so that at present will not be further discuss.

4. Conclusions

The large conjugated π-electrons system that highly stabilises mepanipyrim from fragmentation offers the reason why this molecule is so easily degraded. As a matter of fact, mepanipyrim has been transformed under photocatalytic treatment in air-equilibrated system into numerous species as characterised through a MS^n analysis. The observed intermediates suggest that mepanipyrim can easily be oxidised and/or reduced and that its photodegradation can proceed through both oxidative and reductive pathways, so pointing out that numerous pathways are operating. Several hydroxy- and bihydroxy-mepanipyrim have been identified, further transformed via the loss of propynylic chain, release of the benzenic moiety and so on. Contemporaneously, reduction of the triple bond occurs with the formation of propanolic, propylenic and/or propandiolic structures.

The identified intermediates match those found with metabolic study in soils, while several new species have been found in this laboratory-simulation, that can themselves be formed in treated vegetables.

References

[1] M. Ikeda, Y. Asano, Y. Maeda, Y. Yusa, J. Pest. Sci. 23 (1) (1998) 1.
[2] M. Ikeda, Y. Asano, Y. Maeda, Y. Yusa, J. Pest. Sci. 23 (1) (1998) 9.
[3] Y. Nagai, K. Shimba, Y. Yaga, A. Yagi, J. Pest. Sci. 24 (3) (1999) 280.
[4] M. Nakamura, Y. Kono, A. Takatsuki, Biosci. Biotech. Biochem. 67 (1) (2003) 139.
[5] R.G. Zepp, N.L. Wolfe, Aquatic Surface Chemistry, Wiley, NY, 1987 (Chapter 7).
[6] E. Pelizzetti, C. Minero, V. Maurino, Adv. Colloid Interface Sci. 25 (1991) 460.
[7] A.L. Pruden, D. Ollis, Environ. Sci. Technol. 17 (1983) 628.
[8] C.Y. Hsiao, C.L. Lee, D.F. Ollis, J. Catal. 82 (1983) 418.
[9] T. Hisanaga, K. Harada, K. Tanaka, J. Photochem. Photobiol. A Chem. 54 (1) (1990) 113.
[10] C. Kormann, D. Bahnemann, M.R. Hoffmann, Environ. Sci. Technol. 25 (1991) 494.
[11] F. Sabin, T. Tirlùk, A. Vogler, J. Photochem. Photobiol. A Chem. 63 (1992) 99.

[12] M. Hingendorff, D.W. Bahnemann, J. Adv. Oxid. Technol. 1 (1996) 35.
[13] D.W. Bahnemann, J. Cunningam, M.A. Fox, E. Pelizzetti, P. Pichat, N. Serpone, in: G.R. Helz, R.G. Zepp, D.G. Crosby (Eds.), Surface and Aquatic Photochemistry, Lewis, Boca Raton, FL, 1993, p. 261.
[14] M. Addullah, G.K.C. Low, R.W. Matthews, J. Phys. Chem. 94 (1990) 6820.
[15] C. Minero, G. Mariella, V. Maurino, E. Pelizzetti, Langmuir 16 (6) (2000) 2632.
[16] D. Lawless, N. Serpone, D. Meisel, J. Phys. Chem. 95 (1991) 5166.
[17] S.R. Morrison, Electrochemistry at Semiconductor and Oxidized Metal Electrodes, Plenum, New York, 1980 (Chapter 5).
[18] M.R. Hoffmann, S.T. Martin, W. Choi, D.W. Bahnemann, Chem. Rev. 95 (1995) 69.
[19] C. Von Sonntag, et al., in: M.G. Simic (Ed.), Oxygen Radicals in Biology and Medicine, Plenum Press, New York, 1988, p. 47.
[20] A. Kunai, S. Hata, S. Ita, K. Sasaki, J. Am. Chem. Soc. 108 (1986) 6012.
[21] P. Calza, C. Medana, C. Baiocchi, E. Pelizzetti, Appl. Catal. B Environ. 52 (4) (2004) 267.
[22] R. Terzian, N. Serpone, C. Minero, E. Pelizzetti, J. Catal. 128 (1991) 352.
[23] E. Pelizzetti, C. Minero, V. Maurino, Adv. Colloid Interface Sci. 21 (1990) 271.
[24] V. Maurino, C. Minero, E. Pelizzetti, P. Piccinini, N. Serpone, H. Hidaka, J. Photochem. Photobiol. A Chem. 109 (2) (1997) 171.
[25] S. Horikoshi, N. Watanabe, M. Mukae, H. Hidaka, N. Serpone, New J. Chem. 25 (8) (2001) 999.
[26] P. Piccinini, C. Minero, M. Vincenti, E. Pelizzetti, Catal. Today 39 (1997) 187.
[27] S. Horikoshi, H. Hidaka, J. Photochem. Photobiol. A Chem. 141 (2001) 201.
[28] E. Pelizzetti, C. Minero, E. Borgarello, L. Tinucci, N. Serpone, Langmuir 9 (1993) 2995.